JOURNAL OF BACTERIOLOGY, Sept. 1992, p. 5827–5839
0021-9193/92/185827-13$02.00/0

Vol. 174, No. 18

Localization of a *Porphyromonas gingivalis* 26-Kilodalton Heat-Modifiable, Hemin-Regulated Surface Protein Which Translocates across the Outer Membrane

THOMAS E. BRAMANTI† AND STANLEY C. HOLT*

Department of Periodontics, University of Texas Health Science Center at San Antonio, 7703 Floyd Curl Drive, San Antonio, Texas 78284-7894

Received 10 December 1991/Accepted 6 July 1992

We recently identified a 26-kDa hemin-repressible outer membrane protein (Omp26) expressed by the periodontal pathogen *Porphyromonas gingivalis*. We report the localization of Omp26, which may function as a component of a hemin transport system in *P. gingivalis*. Under hemin-deprived conditions, *P. gingivalis* expressed Omp26, which was then lost from the surface after a shift back into hemin-rich conditions. Experiments with ^{125}I labeling of surface proteins to examine the kinetics of mobilization of Omp26 determined that it was rapidly (within <1 min) lost from the cell surface after transfer into a hemin-excess environment. When cells grown under conditions of hemin excess were treated with the iron chelator 2,2′-bipyridyl, Omp26 was detected on the cell surface after 60 min. One- and two-dimensional sodium dodecyl sulfate-polyacrylamide gel electrophoresis and immunoblot analyses using purified anti-Omp26 monospecific polyclonal immunoglobulin G antisera established that Omp26 was heat modifiable (39 kDa unheated) and consisted of a single protein species. Immunogold labeling of negatively stained and chemically fixed thin-section specimens indicated that Omp26 was associated with the cell surface and outer leaflet of the *P. gingivalis* outer membrane in hemin-deprived conditions but was buried in the deeper recesses of the outer membrane in hemin-excess conditions. Analysis of subcellular fractions of *P. gingivalis* grown either in hemin-excess or hemin-deprived conditions detected Omp26 only in the cell envelope fraction, not in the cytoplasmic fraction or culture supernatant. Limited proteolytic digestion of hemin-deprived *P. gingivalis* with trypsin and proteinase K verified the surface location of Omp26 as well as its susceptibility to proteolytic digestion. Heat shock treatment of hemin-excess-grown *P. gingivalis* also resulted in Omp26 translocation onto the outer membrane surface even in the presence of hemin. Furthermore, hemin repletion of heat-shocked, hemin-deprived *P. gingivalis* did not result in Omp26 translocation off the outer membrane surface, suggesting that thermal stress inactivates this transmembrane event. This newly described outer membrane protein appears to be associated primarily with the outer membrane, in which it is exported to the outer membrane surface for hemin binding and may be imported across the outer membrane for intracellular hemin transport.

In response to iron limitation, prokaryotes express outer membrane proteins (Omps) that may participate in the binding and uptake of iron from the external milieu (11, 40). Upon entry into a vertebrate host, a bacterium encounters an iron-restricted habitat in which iron is either sequestered within intracellular compartments or tightly bound to partially saturated host iron-binding proteins (12, 41). These iron-sequestering systems are critical components of host defenses directed against bacterial infection and function to limit the ability of microbial pathogens to reside, or to grow and emerge, within the host.

The periodontal pathogen *Porphyromonas gingivalis* is capable of circumventing the host's iron-withholding defenses by incorporating host-associated iron into its own metabolic machinery (6). Functionally, the highly proteolytic nature of *P. gingivalis* (18) contributes to the destruction of host iron-binding proteins (i.e., transferrin, lactoferrin, albumin, and hemoglobin), thereby releasing their bound iron and heme into the environment of the periodontal pocket, where they can be utilized by *P. gingivalis* and other members of this ecosystem. The released iron and heme are scavenged by *P. gingivalis* Omps and processed for cellular metabolism (6).

To date, iron and hemin uptake mechanisms have not been identified in *P. gingivalis* or in any of the other oral pathogens. Previous studies (5, 7) suggest that a 26-kDa Omp (Omp26), along with several other Omps that are exposed at the surface of *P. gingivalis*, might be involved in processing hemin-associated iron. These observations revealed that when *P. gingivalis* was grown with limited hemin or was deprived of hemin for extended periods, these proteins were expressed on the outer membrane surface, with Omp26 being the predominant surface protein (5, 7). Important in ascribing a function to Omp26, transfer of hemin-deprived *P. gingivalis* into an environment of excess hemin resulted in loss of Omp26 from the cell surface, implying some participation of this protein in hemin uptake by *P. gingivalis* (7).

Although it is well established that Omp26 is located on the surface of the *P. gingivalis* outer membrane in hemin-deprived conditions (5, 7), the physical and biochemical mechanisms by which Omp26 responds to the presence and absence of hemin are not known. We previously established that the *P. gingivalis* Omp26 was regulated exclusively by an intact hemin molecule and was not affected by other porphyrins or by organic or inorganic sources of iron (7). Movement or loss of Omp26 from the *P. gingivalis* surface required a cell-associated interaction with a tetrapyrrole porphyrin ring

* Corresponding author.
† Present address: Department of Stomatology, University of California—San Francisco, San Francisco, CA 94143-0650.

which was coordinated specifically with the iron atom; protoporphyrin IX alone or protoporphyrin IX coordinated to zinc did not mobilize Omp26 off the outer membrane surface. The response of Omp26 to hemin and the specificity with which this Omp was regulated provided strong evidence that this protein was involved in hemin acquisition by *P. gingivalis*.

There are no data on the effects of environmental stress(es) other than hemin limitation on Omp26 expression in *P. gingivalis*. In fact, there are very few studies which have identified the effects of multiple environmental stresses on the expression of prokaryotic proteins (4, 20, 28, 36). Members of a well-studied and well-described class of environmental stress proteins, the heat shock proteins (26), are synthesized by both prokaryotic and eukaryotic cells in response to thermal stress. These heat shock proteins are also synthesized by bacteria in response to nutrient deprivation, pH changes, and oxidative levels (4, 20, 28, 36). In *Escherichia coli*, thermal stress induces the rapid translocation of proteins to the outer membrane (42). Whether Omp26 and the other putative hemin-regulated Omps are also regulated by heat shock, and especially their translocation on and off the outer membrane, is unknown.

The purpose of this study was to extend our initial observations (5, 7) on the identification of the hemin-regulated Omp26 of *P. gingivalis* and to determine its location in response to hemin. We report the occurrence of a heat-modifiable 26-kDa macromolecule (39 kDa unheated) which is present on the surface of *P. gingivalis* in response to hemin deprivation and in response to hemin repletion, is lost from the surface, but remains associated with the outer membrane.

MATERIALS AND METHODS

Growth conditions. *P. gingivalis* ATCC 53978 (W50) was maintained as described previously (6). Bacteria were exposed to conditions of hemin excess (7.7 μM) or hemin deprivation in 2.1% (wt/vol) mycoplasma basal broth (BBL, Cockeysville, Md.) as described previously (6).

Heat shock treatment. The effect of heat shock on the expression and mobilization of *P. gingivalis* Omps was examined in cells grown in both hemin-depleted and hemin-replete conditions. Hemin-excess and hemin-deprived cells were grown to mid-logarithmic growth phase, and the growth flask was purged with anaerobic gas and sealed. The culture was heat shocked at 45°C for 30 min in a water bath. To determine the effect of heat shock on Omp repression, hemin-depleted *P. gingivalis* were heat shocked as described above and then exposed to 7.7 μM hemin for 15 min. All cells were harvested and immediately iodinated (see below) and then compared with iodinated control cells grown at 37°C.

Preparation of growth supernatant, outer envelope, cell envelope, and cytoplasmic fractions. Growth supernatants were collected from *P. gingivalis* cultures after centrifugation (14,000 × *g*, 30 min) to remove whole cells. Spent growth medium was concentrated 20-fold in a Savant Speed-Vac concentrator (Savant Instruments, Inc., Farmingdale, N.Y.) (supernatant fraction). Whole cell pellets were washed in phosphate-buffered saline (PBS; pH 7.2) and then radioiodinated (7). Cell envelope fractions, containing the inner membrane, outer membrane, and peptidoglycan, were prepared by French pressure disruption (5). After high-speed centrifugation (200,000 × *g*, 2 h), soluble extracts from the French pressure-disrupted cells, containing the cytoplasmic fraction, were collected, and the cell envelope pellet was either suspended in distilled H_2O (cell envelope fraction) or treated by a modification of our previously described method (7), using 15 ml of 4% (wt/vol) Sarkosyl for 6 h at 37°C to solubilize the cytoplasmic membrane and collect the insoluble pellet (outer envelope fraction).

Kinetics of mobilization of Omp26. Omp26 was induced to move to the outer membrane surface of *P. gingivalis* by subjecting cells to iron stress. The iron chelator 2,2′-bipyridyl (BPD) was added at 400 μM to cells grown in mycoplasma basal broth containing 7.7 μM hemin (BPD shock). Samples (200 ml) were withdrawn from the growth vessel at various times, cooled to 4°C, and washed in cold PBS; the cells were then iodinated, and their outer envelopes were isolated as described above. To mobilize Omp26 off the *P. gingivalis* cell surface, either hemin-deprived *P. gingivalis* cells were transferred into medium containing an excess of hemin or BPD-shocked cells were washed in sterile PBS and transferred into medium containing excess hemin but no BPD. Aliquots were withdrawn at selected times and immediately cooled to 4°C in a cold ethanol bath. Cells were then kept at 4°C and iodinated, their outer envelopes were isolated, and the kinetics of movement of Omp26 from the outer membrane surface was determined by sodium dodecyl sulfate (SDS)-polyacrylamide gel electrophoresis (PAGE) and autoradiography as described below.

1-D and 2-D SDS-PAGE. One-dimensional and two-dimensional (1-D and 2-D) SDS-PAGE (5, 24) of both control unlabeled and iodinated Omps was performed in both 10 and 12% acrylamide concentrations. The 2-D PAGE routinely employed 10% acrylamide gels and unheated samples in the first dimension (24). Separation of the polypeptides in the second dimension was carried out after boiling of the gel strip from the first dimension and application to the top of a 12% acrylamide gel in the second dimension. Polypeptides were demonstrated by Coomassie brilliant blue (CBB) R-250 stain, and iodinated Omps were demonstrated by autoradiographic analysis (24).

Production of monospecific antibody to Omp26. Since it was difficult to separate Omp26 in preparative SDS-polyacrylamide gels without contamination of small amounts of closely migrating Omps, we used the unheated 39-kDa protein (heated = 26-kDa protein), which was readily separated and purified by 1-D and 2-D SDS-PAGE, for monospecific antibody production. Since the Omp26 and Omp39 polypeptides were identical (see Results), we refer to the antibody prepared against the 39-kDa unheated protein antigen as anti-Omp39 antiserum. Briefly, unheated cell envelope proteins were separated by SDS-PAGE (see above), and Omp39 was excised from the acrylamide gel (12 by 15 cm) (25). The polypeptide was demonstrated by CBB stain, and the corresponding regions of unstained acrylamide strips (0.5 by 15 cm) were cut into small fragments and sheared through an 18-gauge needle in 3 ml of sterile H_2O. This protein (ca. 200 μg/ml) was combined with 1 ml of incomplete Freund's adjuvant and mixed completely. BALB/c mice (female, approximately 20 g, 5 to 8 weeks old) and New Zealand White rabbits (female, 3 to 4 kg) were immunized subcutaneously in the dorsal region with 0.2 ml (mice) or 2 ml (rabbits) of the protein-incomplete Freund's Adjuvant complex. Both groups of animals were immunized three to four times at 2-week intervals. Immune sera were collected and stored at −20°C. Preimmune and immune sera were tested for reactivity to both the heated Omp26 and unheated Omp39 moieties by immunoblotting (see below).

Antibody purification. Both mouse and rabbit anti-Omp39

antisera were initially purified by ammonium sulfate precipitation, and the semipurified immunoglobulin G (IgG) fraction was applied to an Immunopure Protein A/G column (Pierce, Rockford, Ill.) according to the protocol described by Pierce. The purified IgG was collected in 1-ml fractions, and the protein content was measured at 280 nm. Antibody purity was assessed by SDS-PAGE analysis, and its monospecificity was determined by 1-D and 2-D immunoblotting experiments against cell envelope fractions of hemin-deprived *P. gingivalis* (see below).

Immunoblotting. Cell envelope proteins were separated by 1-D and 2-D SDS-PAGE with and without sample boiling. The separated polypeptides were electroblotted onto nitrocellulose paper (0.2-μm pore size) at 100 mA for 5 h by the method of Towbin et al. (38). Antisera to Omp39 or preimmune sera were diluted (1:500, rabbit; 1:200, mouse) in Tris-buffered saline (TBS; 0.05 M Trizma-HCl, 0.9% NaCl, pH 7.5), applied to the blots, and incubated overnight at 25°C on a rocker. The blots were washed, goat anti-rabbit or goat anti-mouse IgG conjugated to horseradish peroxidase (Sigma, St. Louis, Mo.) (1:2,000 dilution in TBS) was applied, and the mixture was incubated for 6 h at 25°C with agitation. The blots were developed with 60 mg of 4-chloro-1-naphthol in 20 ml of cold methanol added to 100 ml of TBS containing 0.1% H_2O_2.

Immunoelectron microscopy. The subcellular distribution of Omp26 in *P. gingivalis* was determined by immunogold localization in negatively stained transmission electron micrographs after chemical fixation and thin sectioning.

(i) **Negative staining.** Hemin-deprived and hemin-excess-grown *P. gingivalis* whole cells were applied to Formvar-coated nickel grids, and excess liquid was drawn off. This procedure was followed by addition of 30 μl of 4% bovine serum albumin (BSA), incubation for 30 min, and then incubation with 30 μl of 0.02 M glycine for 30 min. Omp26 was detected by immunogold labeling (see below), and negative staining was performed by addition of 1% (wt/vol) phosphotungstic acid (pH 7.2) for 10 s.

(ii) **Thin sectioning.** *P. gingivalis* identical to that prepared for negative staining was used for chemical fixation-immunogold localization. Hemin-deprived and hemin-excess-grown *P. gingivalis* cells were fixed in 2% (vol/vol) glutaraldehyde in 0.1 M cacodylate buffer (pH 7.2) for 1 h at 25°C. The glutaraldehyde was removed, and the cells were washed at least three times with cacodylate buffer. The cell pellets were then dehydrated through a graded ethanol and LR-Gold series (2) and embedded in LR-Gold. The plastic was allowed to polymerize at 4°C under UV light for 24 h and then at 25°C for 48 h. Thin sections were prepared on a Sorvall MT-5000 ultramicrotome (Ivan Sorvall, Inc., Norwalk, Conn.), transferred to nickel grids, and incubated with 30 μl of 4% (wt/vol) BSA and 0.02 M glycine for 30 min each to block any nonspecific protein-binding sites. Omp26 was detected by immunogold labeling (see below), and specimens were stained with uranyl acetate and lead citrate (34).

(iii) **Immunogold labeling.** Either mouse preimmune or mouse immune anti-Omp39 antibody was diluted to an appropriate working dilution and reacted with the specimens for 15 min. The grids were then washed three times with PBS containing 1% (wt/vol) BSA and reacted with goat anti-mouse IgG conjugated to 10-nm gold particles (Amersham, Arlington Heights, Ill.) plus 1% (wt/vol) BSA for 15 min. The reaction was stopped by washing the grids with PBS at least three times for 1 min each wash.

All specimens were examined in a JEOL 1200 EX transmission electron microscope operating at 70 kV.

Exposure of Omp26 to proteases. Titrated levels of trypsin (0.01, 0.1, and 1 mg/ml) and proteinase K (1, 10, and 100 μg/ml) suspended in PBS were added to iodinated and unlabeled *P. gingivalis* cell suspensions (3.5×10^{10} cells per ml in PBS), which were incubated at 37°C for 45 min. Proteolytic digestion was stopped by the addition of a protease inhibitor cocktail consisting of *N*-α-*p*-tosyl-L-lysine chloromethyl ketone, benzamidine, and phenymethylsulfonyl fluoride (15 μM each) (5, 24). The treated cells were immediately cooled to 4°C, their cell envelopes were isolated, and proteolytic digestion of Omp26 was examined by SDS-PAGE and autoradiography as described above. In pulse-chase experiments, ^{125}I-labeled and unlabeled *P. gingivalis* cells were washed once in PBS, hemin (7.7 μM) was added, and then the whole cells were treated with proteinase K (100 μg/ml) or trypsin (1 mg/ml) as described above. The location of Omp26 in protease-treated *P. gingivalis* cells as a function of hemin exposure was also examined by immunoblot analysis, using anti-Omp39 antiserum against cell envelope protein antigens from both hemin-deprived and hemin-excess-grown cells.

Protein determination. Total protein was determined by using the bicinchoninic acid assay (Pierce) (24).

RESULTS

Hemin-regulated surface mobilization of Omp26. Our previous observations have unequivocally established that *P. gingivalis* expresses Omp26 on its outer membrane surface when grown in hemin-restricted environments (5, 7). In the presence of excess hemin (7.7 μM), this protein was lost from the outer membrane surface. We have now examined the kinetics of mobilization of Omp26 in response to hemin repletion in an attempt to determine how rapidly this protein is lost from the *P. gingivalis* cell surface in the presence of excess hemin (Fig. 1). ^{125}I-surface-labeled *P. gingivalis* outer envelope fractions from cells grown in conditions of hemin excess revealed that while Omp26 was exposed (Fig. 1A, lane 2), it was significantly reduced at the cell surface in comparison with cells grown in conditions of hemin starvation (Fig. 1A, lane 3), in which Omp26 was the dominant surface protein. The kinetics of mobilization of Omp26 in the presence of excess hemin is shown in Fig. 1A, lanes 4 to 6. Transfer of the hemin-deprived *P. gingivalis* (Fig. 1A, lane 3) back into hemin-excess conditions resulted in an almost immediate reduction (approximately 1 min) in the expression of Omp26 on the outer membrane surface (Fig. 1A, lane 4). Five-minute exposure of the cells to the hemin-excess environment essentially eliminated Omp26 from the outer membrane surface (Fig. 1A, lane 6). The rapid loss of Omp26 from the surface of the hemin-deprived *P. gingivalis* in response to a hemin-excess environment suggested that this protein either may be released from the cell surface into the external milieu or may migrate back into the outer membrane, where it becomes inaccessible to the ^{125}I probe.

The effect of BPD shock on the appearance of Omp26 on the *P. gingivalis* surface was examined by autoradiographic analysis of ^{125}I-labeled cells (Fig. 1B). In the presence of excess hemin (Fig. 1B, lane 1), Omp26 was not significantly exposed on the *P. gingivalis* surface, while under hemin-deprived conditions, Omp26 was significantly exposed on the surface (Fig. 1B, lane 2). Addition of a 400 μM concentration of the iron chelator BPD to hemin-excess-grown *P. gingivalis* resulted in maximal surface exposure of Omp26 after a 60-min incubation period (Fig. 1B, lanes 3 to 5) and was comparable to the Omp pattern observed in hemin-

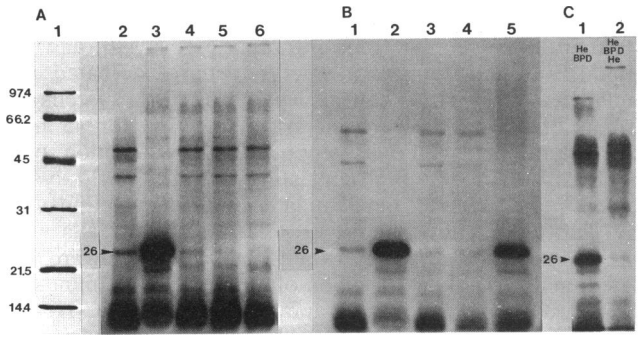

FIG. 1. ^{125}I autoradiographs of Omps from *P. gingivalis* W50. (A) Cells were grown in the presence and absence of hemin. Lanes: 1, positions of molecular mass standards in kilodaltons; 2, cells grown in 7.7 μM hemin; 3, cells deprived of hemin (five passages); 4 to 6, hemin-deprived passage 5 cells transferred into 7.7 μM hemin culture for 1, 3, and 5 min (lanes 4, 5, and 6, respectively). Each lane was loaded with 250,000 cpm. (B) Cells grown in hemin were treated with the iron chelator BPD. Lanes: 1, 7.7 μM hemin-grown cells (negative control); 2, hemin-deprived (passage 5) cells (positive control); 3 to 5, 7.7 μM hemin-grown cells treated with 400 μM BPD for 15 min (lane 3), 30 min (lane 4), and 60 min (lane 5). (C) Omps from cell envelope fractions separated on an ^{125}I autoradiograph which was different from that shown in panel B. Lanes: 1, 7.7 μM hemin-grown cells (He) treated with 400 μM BPD for 60 min; 2, 7.7 μM hemin-grown cells treated with 400 μM BPD for 60 min, washed, and then transferred back into 7.7 μM hemin medium for 5 min. In panels B and C, 150,000 cpm was applied to each lane.

deprived conditions (Fig. 1B, lane 2). The appearance of Omp26 in response to BPD (Fig. 1C, lane 1) could be immediately reversed (i.e., within 5 min) by transfer of the BPD-shocked *P. gingivalis* (after washing in PBS) back into hemin-excess culture in the absence of BPD (Fig. 1C, lane 2).

1-D and 2-D SDS-PAGE and ^{125}I autoradiographic analysis of Omp26. To determine whether Omp26 was a single protein species or represented a comigrating complex of different proteins, we performed 2-D SDS-PAGE analysis of cell envelope fractions (Fig. 2). Heating before separation in the second dimension resulted in the conversion of the 39-kDa species to the 26-kDa form. SDS-PAGE (Fig. 2A) and its identical ^{125}I autoradiograph (Fig. 2B) of Omps from hemin-deprived *P. gingivalis* revealed that Omp26 migrated from a single 39-kDa protein species after heating (Fig. 2A and B, arrows). Although this protein represented the dominant ^{125}I-labeled moiety at this molecular mass (Fig. 2B, large arrowhead), heating of the Omps also resulted in the migration of the heat-modified polypeptides comprising the 24-kDa triplet from 45-, 48-, and 52-kDa species, respectively (Fig. 2B, small arrowheads). The 24-kDa protein was separated from the closely migrating Omp26 in 12% or greater acrylamide concentrations (Fig. 2B, vertical inset).

Characterization of the monospecific polyclonal anti-Omp39 antisera. IgG affinity purification elution profiles of both mouse and rabbit anti-Omp39 antisera exhibited a single protein peak, consisting of a homogeneous antibody preparation as determined by SDS-PAGE (data not shown). In immunoblot analyses, both the rabbit (Fig. 3) and mouse (data not shown) anti-Omp39 antisera were immunologically reactive with the heated 26-kDa and unheated 39-kDa proteins (Fig. 3, lanes 2 and 3, respectively). Since the immunoblot analysis revealed a more intense immunoreactivity against the 39-kDa unheated form of the protein, the results presented here are those obtained from immunoblot analyses of unheated *P. gingivalis* cell envelope fractions (Fig. 4). Omp39 was also detected in SDS-polyacrylamide gels of the unheated *P. gingivalis* cell envelope fractions from both

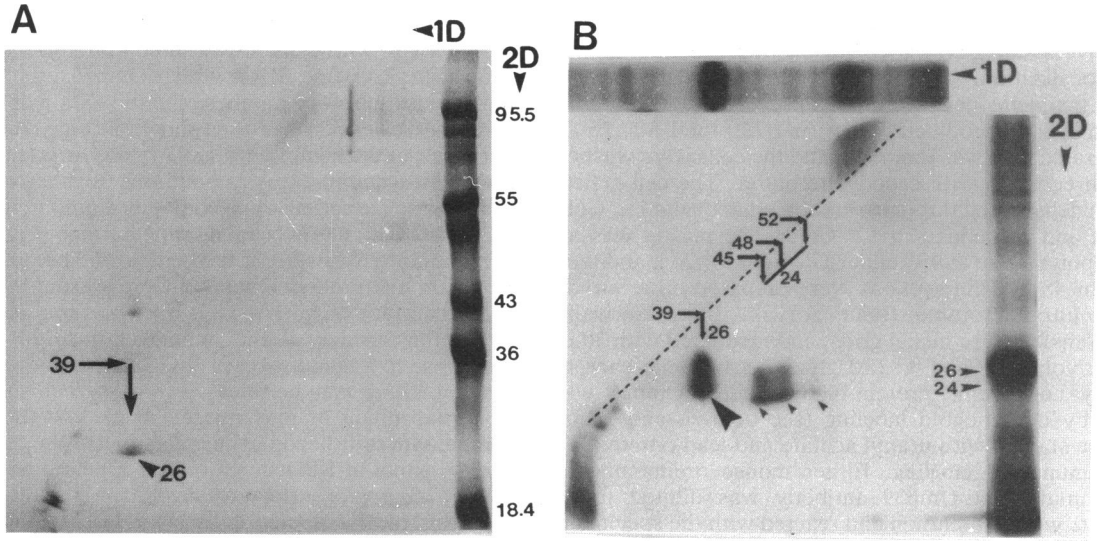

FIG. 2. Two-dimensional SDS-PAGE (A) and ^{125}I autoradiography (B) of *P. gingivalis* W50 heat-modifiable Omps from hemin-deprived cells. A 100-μg sample of protein (A) and 250,000 cpm of hemin-deprived (passage 5) cell envelope fraction (B) was applied to a 10% acrylamide gel in the first dimension without heating (the 1-D unheated profile of ^{125}I-labeled Omps is shown in the horizontal inset in panel B). The lane was excised, heated at 100°C for 5 min, and juxtaposed horizontally on a 12% acrylamide second-dimension gel. 1-D profiles of ^{125}I-labeled heated cell envelope fractions are seen in the vertical inset in panel B. Heat-modifiable proteins migrated above and below the diagonal profile. Molecular mass standards in kilodaltons are shown on the right side of the SDS-polyacrylamide gel (A). Arrows indicate points of intercept across the diagonal and the corresponding molecular masses in kilodaltons. Arrowheads indicate locations of Omp26 and Omp24 triplets (B). 1D, first dimension; 2D, second dimension.

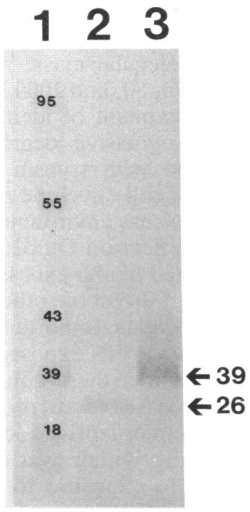

FIG. 3. Immunoblot analysis of *P. gingivalis* W50 heat-modifiable Omp39 (Omp26). A 10% acrylamide concentration was used for polypeptide separation. Lanes: 1, prestained molecular mass standards in kilodaltons; 2 and 3, cell envelope fractions of hemin-deprived cells, which were boiled (lane 2, Omp26) or not boiled (lane 3, Omp39) before analysis. A 100-μg sample of protein was applied to each lane, and the immunoblot was reacted with monospecific rabbit anti-Omp39 antiserum (1:500 dilution). The molecular masses of Omp26 and Omp39 in relation to the protein standards were calculated by linear regression.

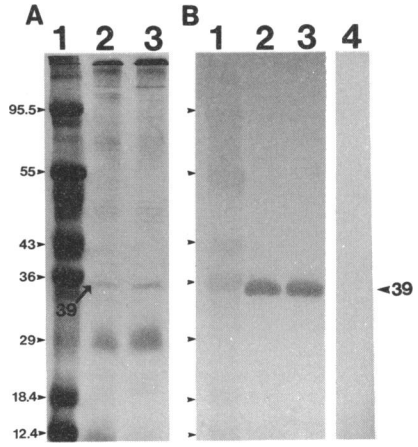

FIG. 4. SDS-PAGE (CBB-stained gel) (A) and immunoblot (B) of *P. gingivalis* W50 cell envelopes from hemin-deprived and hemin-excess-grown cells. A 100-μg sample of unheated cell envelope protein was applied to each lane. Lanes: 1, prestained molecular mass standards in kilodaltons; 2, cell envelopes of 7.7 μM hemin-grown cells; 3 and 4, cell envelopes of hemin-deprived cells (passage 5). The immunoblot (B) was reacted with monospecific rabbit anti-Omp39 antiserum (1:1,000 dilution) (lanes 2 and 3) or rabbit preimmune serum (1:500 dilution) (lane 4). Arrowheads on left side of panel B indicate molecular mass standards (in kilodaltons) corresponding to those seen in panel A, lane 1. Large arrowhead and arrow indicate locations of the 39-kDa protein. The molecular mass of Omp39 was estimated by linear regression.

hemin-excess-grown (Fig. 4A, lane 2) and hemin-deprived (Fig. 4A, lane 3) cells; importantly, it appeared to be quantitatively similar in its distribution in the cell envelope fractions from these two environmental conditions. Immunoblot analysis (Fig. 4B) of identical fractions also revealed immunologic reactivity to Omp39 in both hemin-replete and hemin-deprived cell envelope fractions (Fig. 4B, lane 2 and 3, respectively). No immunoreactivity to *P. gingivalis* cell envelope proteins was observed with rabbit preimmune serum (Fig. 4B, lane 4). The rabbit and murine immune antisera and preimmune sera demonstrated identical immunoreactivity profiles (data not shown). 2-D immunoblot analysis also revealed the monospecificity of the anti-Omp39 antisera (data not shown). As in Fig. 2A, the heat-modified 26-kDa protein seen in the 2-D SDS-polyacrylamide gel migrated from its relative molecular mass of 39 kDa after heating and was immunoreactive with both rabbit and murine purified anti-Omp39 antisera. Thus, it is likely that the polyclonal monospecific IgG anti-Omp39 antiserum is directed against homologous protein antigens in *P. gingivalis* with relative molecular masses at 39 and 26 kDa.

Distribution of Omp26 (Omp39) in subcellular fractions of *P. gingivalis*. We confirmed the presence of Omp26 in the cell envelope of *P. gingivalis* by immunological analysis of the fractionated envelope after French pressure disruption (Fig. 5). The *P. gingivalis* cultures were separated into a soluble growth supernatant, a French pressure-separated cell envelope fraction, and a soluble cytoplasmic fraction. These preparations were reacted in immunoblot analyses with anti-Omp39 antiserum (Fig. 5). We found that the anti-Omp39 antibody reacted with the unheated cell envelope fractions from *P. gingivalis* grown in both hemin-deprived (Fig. 5, lane 7) and hemin-excess (Fig. 5, lane 4) conditions. However, it did not recognize the Omp39 antigen in the soluble cytoplasmic fraction (Fig. 5, lanes 3 and 6) or in the growth culture supernatants (Fig. 5, lanes 2 and 5) from either of these growth conditions. Note that a 50-kDa cross-reactive antigen was observed in the soluble cytoplasmic fraction of hemin-deprived *P. gingivalis* (Fig. 5, lane 6) but not in the corresponding fraction of hemin-replete cells (Fig. 5, lane 3). This 50-kDa protein might possibly represent a de novo intracellular product destined for export across the inner membrane or may be an unprocessed precursor of Omp39. Preimmune rabbit serum did not react with hemin-deprived cell envelope proteins (Fig. 5, lane 1) or with cytoplasmic and supernatant fractions (data not shown). Rabbit (Fig. 5) and mouse (data not shown) immune and preimmune sera reacted identically.

Immunogold localization of Omp26 (Omp39) in *P. gingivalis*. Transmission electron microscopy with immunogold labeling was used to localize Omp26 in intact *P. gingivalis* (Fig. 6). Mouse polyclonal monospecific anti-Omp39 antisera combined with negative staining of specimens of *P. gingivalis* grown under hemin-deprived conditions revealed an even distribution of gold particles on the cell surface (Fig. 6A). Transfer of these hemin-deprived cells into excess hemin for only 5 min resulted in essentially no gold labeling of the surface of hemin-replete cells with anti-Omp39 antibody (Fig. 6B).

Thin sections of *P. gingivalis* grown under hemin-deprived and hemin-excess conditions were also subjected to immunogold localization of Omp39 (Fig. 6C and D, respectively). Under hemin deprivation (Fig. 6C), the anti-Omp39 antiserum label was found almost exclusively in the cell envelope, with most of the gold label being associated with the cell surface and outer membrane layers (arrows). Transfer of these hemin-deprived cells into hemin-excess conditions (Fig. 6D) reversed this pattern; the gold label was only sparsely distributed on the cell surface, with much of it appearing to be buried in the cell envelope (arrows). In the

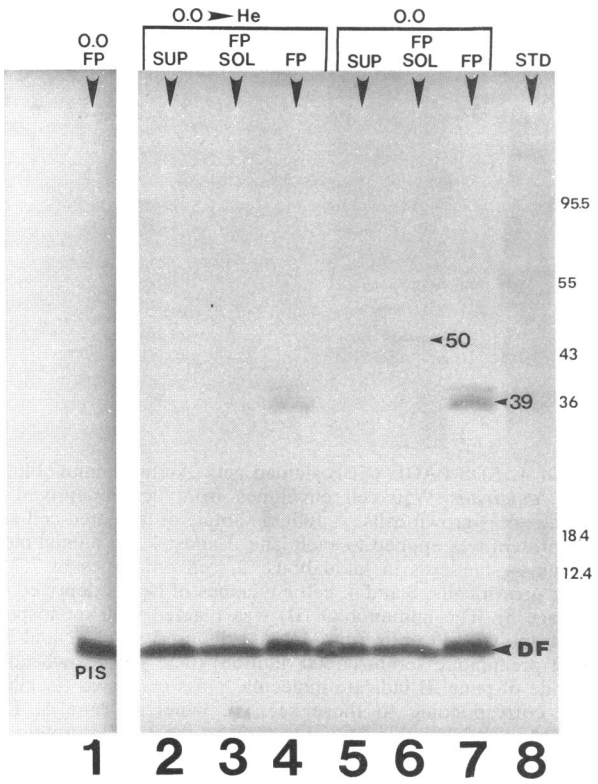

FIG. 5. Immunoblot detection of Omp39 (Omp26) in *P. gingivalis* W50 subcellular fractions by using anti-Omp39 antiserum. A 100-μg sample of protein was applied to each lane. Purified monospecific rabbit anti-Omp39 antiserum (1:1,000 dilution) (lanes 2 to 8) or rabbit preimmune serum (1:500 dilution) (PIS; lane 1) was applied to soluble growth supernatant (SUP), soluble cytoplasmic fraction of French pressure-disrupted cells (FP/SOL), and cell envelope fraction (FP) of hemin-replete (0.0 → He; lanes 2 to 4) and hemin-deprived (0.0; lanes 5 to 7) *P. gingivalis* W50. Lane 8, prestained molecular mass standards (STD) in kilodaltons. DF, dye front.

presence of preimmune mouse serum, no outer membrane-associated immunogold label was observed in either the negatively stained specimens or the thin sections (data not shown). While we were not able to determine unequivocally the exact location of Omp26 by immunogold labeling, we were able to demonstrate a clear difference in distribution of the label in the *P. gingivalis* cells grown under these two environmental conditions (compare Fig. 6C with Fig. 6D).

Proteolytic digestion of Omp26 on the surface of *P. gingivalis*. Exposure of ^{125}I-surface-labeled and unlabeled *P. gingivalis* whole cells to proteolytic digestion was used to ascertain whether Omp26 was exposed at the outer membrane surface during hemin deprivation and migrated to the deeper recesses of the outer membrane (i.e., into the cell envelope) when hemin was replenished (Fig. 7 to 10). SDS-polyacrylamide gels of cell envelopes from hemin-deprived *P. gingivalis* exposed to increasing concentrations of trypsin indicated a progressive degradation of Omp26 (Fig. 7A, lanes 2 to 4) in comparison with untreated control cells (Fig. 7A, lane 1). The proteolytic digestion also resulted in the appearance of several additional protein bands, many of which predominated in the >50-kDa range (Fig. 7A, lanes 3 and 4). ^{125}I autoradiographs of these trypsin-treated *P. gingivalis* cells (Fig. 7B) revealed a significant reduction in the ^{125}I-surface-labeled Omp26 (Fig. 7B, lanes 2 to 4). As in the SDS-polyacrylamide gel (Fig. 7A), there was also an increase in the high-molecular-mass ^{125}I-labeled surface-exposed proteins at 62, 76, 80, and 100 kDa (Fig. 7B, lanes 3 and 4). Proteinase K treatment of identical cell envelopes also resulted in the progressive degradation of Omp26, similar to that observed with trypsin (data not shown). However, SDS-PAGE of cell envelope proteins of *P. gingivalis* grown in a hemin-excess environment revealed trypsin to have no measurable effect on Omp26 (Fig. 8, lane 3) in comparison with untreated hemin-excess control cells (Fig. 8, lane 2). It did, however, digest the other higher-molecular-mass outer membrane proteins. Importantly, Omp26 was not detected in hemin-deprived cells exposed to trypsin (Fig. 8, lane 4), suggesting that under these conditions the surface-exposed Omp26 was accessible to proteolytic action. In contrast, transfer of hemin-deprived cells into a hemin-replete condition (causing withdrawal of Omp26 into the outer membrane) prior to exposure to trypsin resulted in protection of Omp26 from the action of trypsin (Fig. 8, lane 6) in comparison with untreated hemin-replete control cells (Fig. 8, lane 5). As was found for Omp39 (Fig. 4), no differences in the levels of CBB-stained Omp26 were observed in the cell envelopes of *P. gingivalis* when *P. gingivalis* was grown under hemin-excess (Fig. 8, lane 1), hemin-replete (Fig. 8, lane 5), or hemin-deprived (Fig. 8, lane 7) conditions.

The susceptibility of Omp39 to proteolytic action was also examined in immunoblot analyses of proteinase K-treated *P. gingivalis* (Fig. 9). Anti-Omp39 antiserum detected Omp39 in cell envelopes from hemin-deprived and hemin-excess-grown cells (Fig. 9, lanes 1 and 3, respectively); however, exposure of hemin-deprived cells to proteinase K resulted in the degradation of Omp39 (Fig. 9, lane 2), whereas proteinase K had no measurable effect on Omp39 in hemin-excess cells (Fig. 9, lane 4).

We also examined the susceptibility of Omp26 to ^{125}I labeling and proteinase K degradation in hemin pulse-chase experiments (Fig. 10) to confirm the retraction of Omp26 off the cell surface into the deeper recesses of the outer membrane when cells were grown in the presence of hemin. In hemin-deprived *P. gingivalis*, Omp26 was exposed on the surface and was radioiodinated (Fig. 10, lane 1). When transfer of hemin-deprived cells into hemin-replete conditions was followed by ^{125}I labeling, there was no incorporation of ^{125}I into Omp26, indicating the surface loss of this protein (Fig. 10, lane 3). However, when iodination of Omp26 in hemin-deprived cells (pulse) preceded hemin repletion (chase), Omp26 remained radiolabeled, indicating that it had become protected from degradation by proteinase K (Fig. 10, lane 2), and this iodinated protein was buried in the cell envelope after the addition of hemin. Proteinase K treatment of iodinated hemin-deprived cells that were not replenished with hemin resulted in the elimination of the ^{125}I-labeled Omp26 (Fig. 10, lane 4).

Heat shock effects on Omp26 surface expression. Since thermal stress has been reported to induce the translocation of proteins to the outer membrane layer of *E. coli* (42), we examined the effect of heat shock on Omp translocation in hemin-excess-grown *P. gingivalis*, in which Omp26 is not exposed on the outer membrane surface (Fig. 11). Hemin stress (i.e., hemin starvation, positive control) resulted in the appearance of Omp26 on the *P. gingivalis* outer membrane surface (Fig. 11A and B, lanes 1). Exposure of the hemin-excess cells (Omp26 absent from the surface) to heat shock resulted in the appearance of Omp26 on the outer

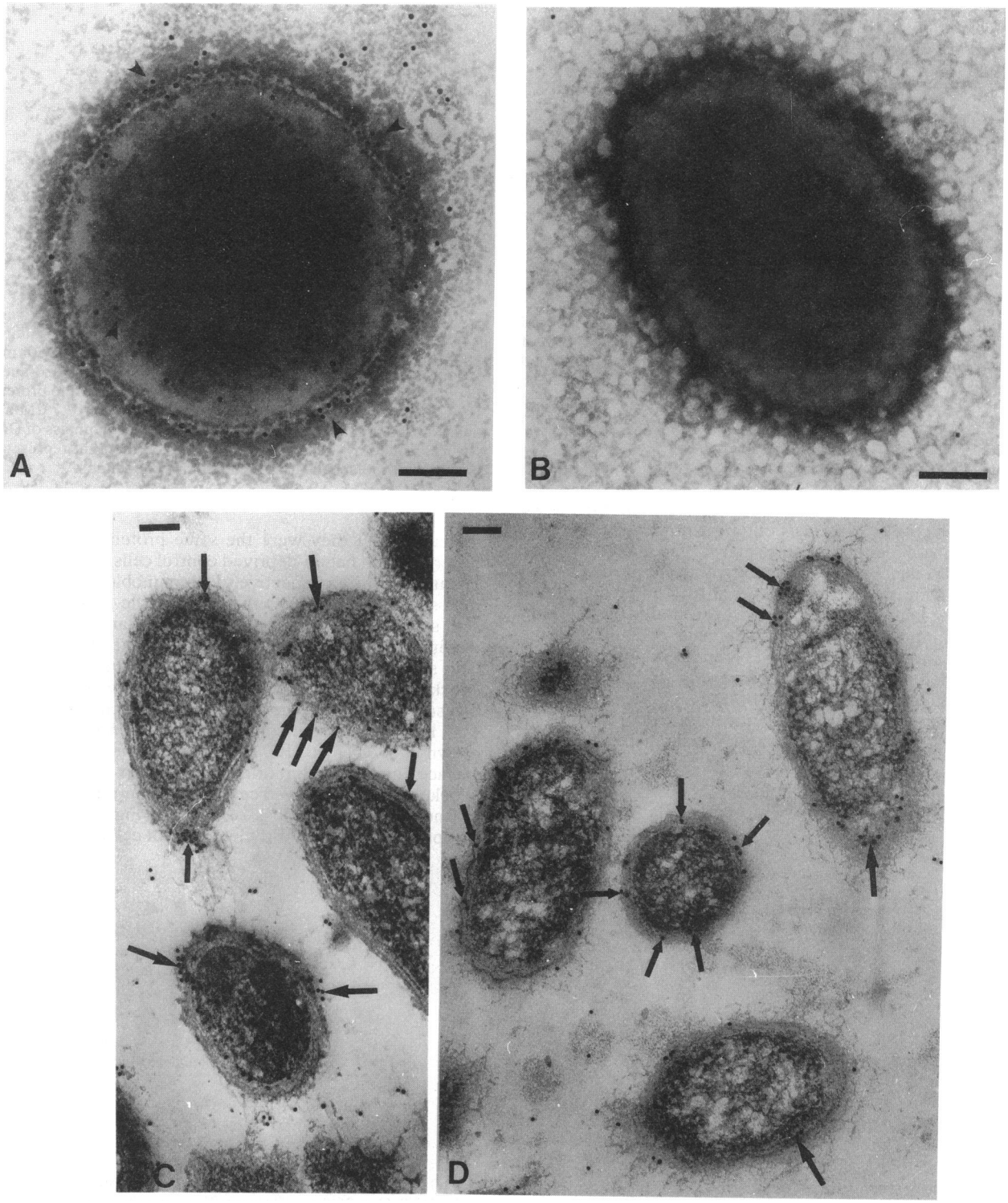

FIG. 6. Immunogold localization of *P. gingivalis* W50 Omp39 (Omp26). Electron photomicrographs of negatively stained *P. gingivalis* cells. (A) Hemin-deprived (passage 6) cells. (B) Hemin-deprived cells which were transferred into 7.7 μM hemin-excess culture for 5 min. *P. gingivalis* cells were incubated with mouse anti-Omp39 antibody followed by anti-mouse IgG conjugated to 10-nm gold. Magnification, ×50,000. (C and D) Thin-section photomicrographs of *P. gingivalis* grown under hemin-deprived (C) and hemin-replete (D) conditions. In cells grown under hemin-deprived conditions (C), the gold–anti-Omp39 label was distributed almost exclusively in the cell envelope. Note that a large amount of the gold label was found associated with the cell surface and outer aspect of outer membrane (arrows). In contrast, *P. gingivalis* grown under hemin-excess conditions (D) showed a significant reduction in the amount of surface label. The gold–anti-Omp39 label appeared to be buried in the outer membrane associated with the inner leaflet (arrows). Panels A through D are representative of an essentially identical distribution of gold label seen in low-magnification electron photomicrographs. Bars = 100 μm.

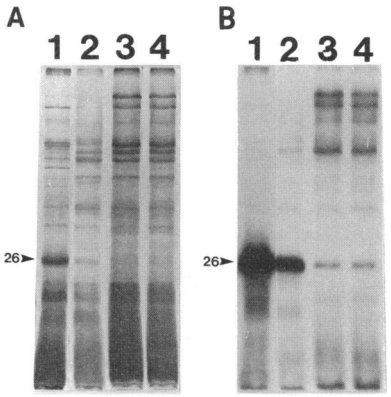

FIG. 7. Trypsin digestion of *P. gingivalis* W50 surface-exposed Omp26. Shown are SDS-PAGE (A) and ^{125}I autoradiograph (B) of cell envelope fractions from hemin-deprived cells (lanes 1, untreated controls) which were incubated with trypsin at 10 (lane 2), 100 (lane 3), or 1,000 (lane 4) μg/ml. Lanes 1 to 4 are identical for panels A and B; 100 μg of protein per lane was loaded in panel A, and 100,000 cpm per lane was applied in panel B.

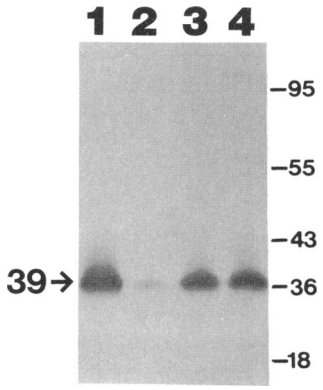

FIG. 9. Immunoblot analysis of proteinase K-treated *P. gingivalis* W50. A 100-μg sample of *P. gingivalis* cell envelope protein was applied to each lane, and the immunoblot was reacted with monospecific mouse anti-Omp39 antiserum (1:1,000 dilution). Lanes: 1, hemin-deprived cells; 2, hemin-deprived cells exposed to proteinase K; 3, cells grown in 7.7 μM hemin; 4, cells grown in 7.7 μM hemin and exposed to proteinase K. The relative molecular mass of Omp39 was calculated by linear regression. Bars on the right represent the positions of molecular mass standards in kilodaltons.

membrane surface (Fig. 11A and B, lanes 3). The emergence of Omp26 on the *P. gingivalis* outer membrane surface after heat shock was identical to that seen with hemin deprivation (cf. Fig. 11A and B, lanes 1). Identical to the results shown in Fig. 2, Omp26 which appeared on the outer membrane surface after hemin depletion was a heat-modifiable polypeptide exhibiting a relative molecular mass of 39 kDa in the absence of sample boiling (Fig. 11A and B, lanes 2) and was heat modified to 26 kDa after boiling (Fig. 11A and B, lanes 1). Autoradiographic analysis of the *P. gingivalis* heat-shocked Omps confirmed the identical natures of Omp26 and Omp39 (Fig. 11A and B, lanes 3 and 4, respectively), indicating that they were the same protein species as that observed with hemin-deprived control cells (cf. Fig. 11A and B, lanes 1 and 2, respectively). Immunoblot analysis of the heat-shocked antigens with monospecific anti-Omp39 antisera showed reactivity with both the 26- and 39-kDa Omps, confirming protein identity for both hemin deprivation and heat shock conditions (data not shown). Interestingly, heat shock treatment of hemin-deprived *P. gingivalis* had no measurable effect on the surface appearance of Omp26 (Fig. 11C, lane 2) in comparison with hemin-deprived control cells grown at 37°C (Fig. 11C, lane 1), since Omp26 was already surface exposed. Importantly, transfer of these heat-shocked, hemin-deprived cells into hemin-replete conditions did not result in the loss of Omp26 (Fig. 11C, lane 3) in comparison with hemin-replete control cells which were not

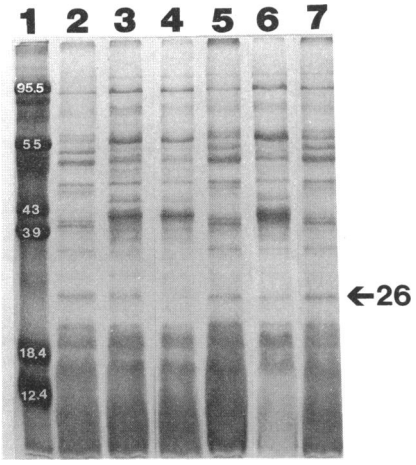

FIG. 8. Susceptibility of *P. gingivalis* W50 Omp26 to trypsin digestion as a function of exposure to hemin. An SDS-polyacrylamide gel of cell envelope proteins from hemin-deprived and hemin-replete *P. gingivalis* W50 cells is shown. Lanes: 1, prestained molecular mass standards in kilodaltons; 2, cells grown in 7.7 μM hemin (untreated control); 3, cells grown in 7.7 μM hemin and exposed to trypsin; 4, hemin-deprived cells exposed to trypsin; 5, hemin-deprived cells transferred into hemin-replete conditions (untreated control); 6, hemin-deprived cells transferred into hemin-replete conditions and then exposed to trypsin; 7, hemin-deprived cells (untreated control).

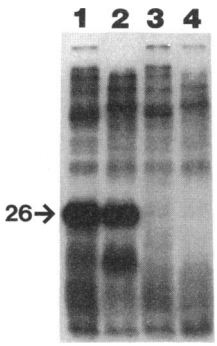

FIG. 10. ^{125}I autoradiograph showing susceptibility of *P. gingivalis* W50 Omp26 to proteinase K in hemin pulse-chase experiments. Each lane of the 12% acrylamide gel was loaded with 300,000 cpm of ^{125}I-surface-labeled *P. gingivalis* cell envelope proteins. Lanes: 1, hemin-deprived cells were iodinated (^{125}I), showing surface expression of Omp26 (positive control); 2, hemin-deprived cells were iodinated, transferred into hemin-replete conditions, and then exposed to proteinase K; 3, hemin-deprived cells were transferred into hemin-replete conditions and then iodinated, showing the absence of Omp26 from the surface (negative control); 4, hemin-deprived cells were iodinated and then exposed to proteinase K.

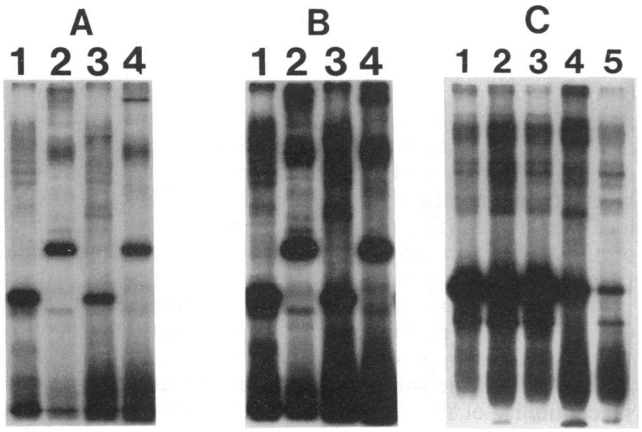

FIG. 11. (A and B) ^{125}I autoradiograph of Omps from *P. gingivalis* W50 exposed to heat shock. Omps were heated at 100°C for 5 min (lanes 1 and 3) or incubated at 37°C for 5 min (lanes 2 and 4) prior to loading on a 12% acrylamide gel; 250,000 cpm was applied to each lane. (A) Lanes: 1 and 2, hemin-deprived cells; 3 and 4, cells grown in 7.7 μM hemin and heat shocked at 45°C for 30 min. (B) Overexposure of the autoradiograph shown in panel A. (C) A 12% acrylamide gel of Omps heated at 100°C for 5 min with 250,000 cpm applied to each lane. Lanes: 1, hemin-deprived control cells; 2, hemin-deprived cells exposed to heat shock conditions; 3, hemin-deprived cells exposed to heat shock and then transferred into hemin-replete conditions; 4, cells grown in 7.7 μM hemin and exposed to heat shock; 5, control cells grown in 7.7 μM hemin.

heat shocked (Fig. 11C, lane 5), suggesting that the mobilization of Omp26 off the *P. gingivalis* outer membrane surface was also inhibited by heat shock in hemin-replete cells (Fig. 11C, lane 4).

DISCUSSION

Hemin is a critical nutrient for growth and metabolism of *P. gingivalis*, since it serves both as a source of iron and as an essential vehicle for iron storage in the cell envelope (6). The mechanism(s) by which *P. gingivalis* binds and transports hemin remains unclear. In vivo, since *P. gingivalis* is associated with inflammatory disease (periodontal disease), it likely obtains its hemin from the hemoglobin stored within erythrocytes. The recent observation of Chu et al. (14) that *P. gingivalis* possesses a potent outer membrane-associated hemolysin supports erythrocyte lysis as a source of hemin for *P. gingivalis*. Once liberated, hemoglobin rapidly combines with serum haptoglobin (41); proteolytic action by *P. gingivalis* on this hemoprotein complex (13) may be its means of securing hemin. Similar to iron transport in other prokaryotic cells (9, 11, 16, 27, 30, 32), binding and transport of hemin by *P. gingivalis* likely occurs by the production of hemin-regulated Omps. Since binding and transport of metabolically required compounds into a bacterial cell may occur through the action of cell surface receptors (10), the investigations presented here examined the appearance and disappearance of surface proteins in response to hemin modulation.

P. gingivalis Omp26 was clearly located on the surface of the cell in a hemin-deprived environment and was very rapidly internalized into the cell envelope when hemin was replenished (Fig. 1). Recently, we also demonstrated that essentially all of the recognized strains of *P. gingivalis* produced a 26-kDa hemin-repressible surface protein which is exposed on the cell surface of hemin-deprived cells (7). Iron-repressible Omps have been identified in a large number of gram-negative prokaryotes (for reviews, see references 11, 16, 27, and 32); however, few of these studies have localized them to the bacterial cell surface. Stugard et al. (37) identified a 101-kDa hemin-binding Omp in *Shigella flexneri* which not only binds hemin but remains expressed on the cell surface in the presence of hemin. A hemin-associated 44-kDa Omp has also been identified in *Bacteroides fragilis* (31); however, it is not known whether this protein is exposed on the cell surface or how it is regulated in response to hemin repletion. Hanson and Hansen (19) have described a 51-kDa hemin-binding lipoprotein in *Haemophilus influenzae*, but the exact location of this protein in the *H. influenzae* cell envelope has not been clearly established. The 49-kDa surface A-layer protein of *Aeromonas salmonicida* has also been shown to bind hemin and porphyrins (23). This 49-kDa surface array protein was constitutively expressed under both high- and low-hemin conditions, and binding of porphyrins to this layer may occur by nonspecific hydrophobic interactions. With *P. gingivalis*, it appears that in response to hemin, the 26-kDa hemin-regulated Omp moved into the cell envelope, remaining primarily associated with the outer membrane. Since Omp26 occurred in cell envelopes at comparable levels under both hemin-deprived and hemin-excess conditions but was found in different locations in the outer membrane, depending upon the presence or absence of hemin (Fig. 4, 5, 8, and 9), it seems that Omp26 is constitutively exhibited in the cell envelope of *P. gingivalis* and that its translocation on and off the outer membrane surface in response to hemin may not require de novo synthesis. To our knowledge, this is the first study to describe the very rapid loss (within <1 min) of a prokaryotic protein from the cell surface in response to an iron-replete environment. Since autologous protein import systems have not been described for gram-negative bacteria, the events responsible for mobilizing Omp26 off the outer membrane surface are unknown.

Although Omp26 was rapidly lost from the surface of hemin-deprived *P. gingivalis* upon transfer into hemin-excess conditions, the reverse process, i.e., surface exposure of Omp26 in hemin-deprived conditions, required a greater amount of time (Fig. 1B). The appearance of Omp26 on the surface of hemin-deprived *P. gingivalis* required at least two serial passages (>10 cell doublings) in hemin-free medium (5). Our previous observations revealed that depletion of the internal hemin stores of *P. gingivalis* coincided with the appearance of Omp26 on the cell surface (5, 7). This delay in the surface exposure of Omp26 was probably due to the utilization of hemin stores by *P. gingivalis* for growth in the hemin-free environment (6). In contrast, iron-limited *Vibrio cholerae* demonstrated iron-regulated Omps 3.5 h after transfer to a low-iron medium (35). Therefore, the appearance of Omp26 on the surface of *P. gingivalis* in response to a hemin-free environment occurs at a much slower rate and may reflect a requirement that the internal hemin stores be depleted before the cell senses this low-hemin environmental stress and begins to translocate Omp26 to the outer membrane surface. When we used the iron chelator BPD (400 μM) to invoke an iron stress in hemin-excess-grown *P. gingivalis*, a more rapid appearance of Omp26 occurred reproducibly after a 60-min incubation. We have reported previously (6) that addition of BPD to *P. gingivalis* cultures simulated an iron-starved environment that inhibited growth, indicating that hemin-associated iron chelation by BPD was easily achieved under anaerobic conditions. De-

neer and Potter (15) have shown that BPD shock (200 μM) of *Actinobacillus pleuropneumoniae* resulted in expression of iron-regulated Omps within 15 min, which represents much faster Omp expression kinetics than we observed with *P. gingivalis*. Although we have no data on the rates of BPD diffusion into the *P. gingivalis* cell, it is likely that surface exposure of the hemin-stress proteins required at least 60 min for diffusion of BPD into the cell and for the complete chelation of internal iron stores. Our findings also suggest that mobilization of Omp26 off the *P. gingivalis* surface was an extremely rapid reversible process, occurring in 5 min or less, once the BPD-induced iron stress was relieved by a shift back to hemin-excess conditions.

As is characteristic of bacterial Omps (3), Omp26 was heat modifiable, migrating with an estimated molecular mass of 39 kDa in the unheated state, which shifted to 26 kDa after boiling. The chromatographically purified, homogeneous, monospecific polyclonal anti-Omp39 IgG antiserum recognized both the heated (Omp26) and unheated (Omp39) antigenic homologs; however, the antiserum showed greater immunoreactivity against Omp39, suggesting it may have a predilection for conformational determinants present in the unheated form of the protein (17). Heating Omp39 in immunoblot analyses may have denatured the predominant conformational determinants recognized by both mouse and rabbit anti-Omp39 antisera, resulting in reduced immunoreactivity to Omp26. Conformation-dependent antibody reactivity has also been reported to occur with hemoglobin, myoglobin, and lysozyme, in which the antigenicity is dependent upon secondary, tertiary, and sometimes quaternary protein conformation (17). Since Omp26 was localized to the *P. gingivalis* outer membrane surface, its protein structure may be similar to that reported for Omps of other gram-negative bacteria, which exhibit heat modifiability and beta-sheet secondary structure (3, 21, 24, 25, 29, 32, 35, 39). Sigel and Payne (35) reported the occurrence of two heat-modifiable iron-regulated cell envelope proteins of 40 and 62 kDa in *V. cholerae* which were peptidoglycan-associated, possibly functioning as porins. Although we have not obtained data on the secondary or tertiary protein structure of Omp26, to our knowledge, this is the first report of a heat-modifiable hemin-regulated Omp.

Use of the purified monospecific anti-Omp39 antibody established that Omp39 was associated with the cell envelope fraction in cells grown in both hemin-replete and hemin-free environments. We therefore conclude that this protein was not released into the extracellular environment or internalized within the cytoplasmic compartment but rather was internalized into the cell envelope. Since the 26- or 39-kDa Omp was not detected in hemin-replete cells by ^{125}I surface labeling or found in any cell fraction other than the cell envelope (Fig. 5), it is highly probable that it was internalized within the outer membrane leaflets of hemin-replete cells.

Immunoelectron microscopic localization of the anti-Omp39–gold conjugates confirmed the location of Omp26 in the *P. gingivalis* cell envelope (Fig. 6). Our findings unequivocally demonstrated that Omp26 was expressed on the surface of negatively stained *P. gingivalis* under hemin-deprived conditions and was lost from the cell surface after a shift to hemin-replete conditions. The loss of Omp26 from the *P. gingivalis* surface upon transfer to a hemin-rich environment was consistent with the very rapid loss of this protein from the *P. gingivalis* surface revealed by the ^{125}I autoradiographic analysis of surface-labeled proteins (Fig. 1). While immunogold localization in chemically fixed thin sections showed that Omp26 predominated in the outer membrane when *P. gingivalis* was starved for hemin, the results for localization of Omp26 under hemin-replete conditions were not as clear as those obtained by negative staining of hemin-replete *P. gingivalis*. However, what was clear was that Omp26 occurred predominantly in the outer membrane layers and not in the cytoplasmic membrane layers or within the cytoplasmic region. The immunogold localization data (Fig. 6) were also consistent with detection of Omp39 by immunoblot localization in the subcellular fractions of *P. gingivalis* (Fig. 5).

To confirm our immunogold localization findings for Omp26, we also performed limited proteolytic digestion of ^{125}I-labeled hemin-deprived *P. gingivalis* cells. These experiments verified the surface location of Omp26 as well as the susceptibility of surface-exposed proteins to proteolytic digestion. CBB-stained SDS-polyacrylamide gels, immunoblot analysis, and ^{125}I autoradiographs of *P. gingivalis* cells exposed to protease (Fig. 8 to 10) established that Omp26 was eliminated in hemin-deprived cells and protected from proteolytic action in hemin-replete conditions. These findings clearly support our hypothesis that Omp26 is retracted into the deeper layers of the outer membrane in response to hemin repletion. Hemin pulse-chase experiments also indicated that the ^{125}I-labeled Omp26 was protected from proteolytic action in hemin-replete conditions and provided further evidence that it remains associated with the cell envelope after translocation off the cell surface (Fig. 10).

Heat shock treatment of hemin-excess-grown *P. gingivalis*, as a stress different from that encountered under hemin deprivation, also resulted in the appearance of Omp26 on the outer membrane surface (Fig. 11). However, in contrast to the hemin-replete-deplete Omp26 mobilization, after heat shock of hemin-replete cells (Omp26 buried within the outer membrane), Omp26 was mobilized to the outer membrane surface (Fig. 11A and B, lanes 3). Exposure of these heat-shocked, hemin-replete or heat-shocked, hemin-deprived *P. gingivalis* cells to hemin did not result in the translocation of Omp26 off the outer membrane surface. Therefore, heat shock apparently initiates Omp26 translocation onto the outer membrane surface but interferes with its mobilization off the outer membrane in the presence of hemin. It is possible that Omp26 or a protein(s) involved in its translocation back into the outer membrane has been structurally altered by the increased temperature, resulting in termination of the Omp26 retraction process(es). Yatvin et al. (42) have reported that when *E. coli* is exposed to thermal stress, proteins undergoing synthesis are rapidly translocated to the outer membrane. As a result of heat shock, global protein synthesis is terminated except for the synthesis of a group of proteins identifiable as chaperonins (heat shock proteins) in the cytoplasm, which function to stabilize cytosolic proteins (26). Chaperonins are not translocated and may not have access to the periplasm and outer membrane compartments (42). In *E. coli*, the translocation of proteins to the outer membrane might counteract the effects of thermal stress and operate to stabilize the outer membrane layer. Translocation of Omp26 onto the *P. gingivalis* surface which results during hemin stress may participate in hemin uptake, since Omp26 is retracted off the surface when hemin is replenished. Heat shock-induced Omp26 translocation may function to stabilize the outer membrane layer remaining exposed on the surface even in the presence of hemin. Immunoblot analysis revealed that both hemin stress and thermal stress result in cell surface induction of the same Omp26, both immunologically and by molecular migration. Multiple environmental

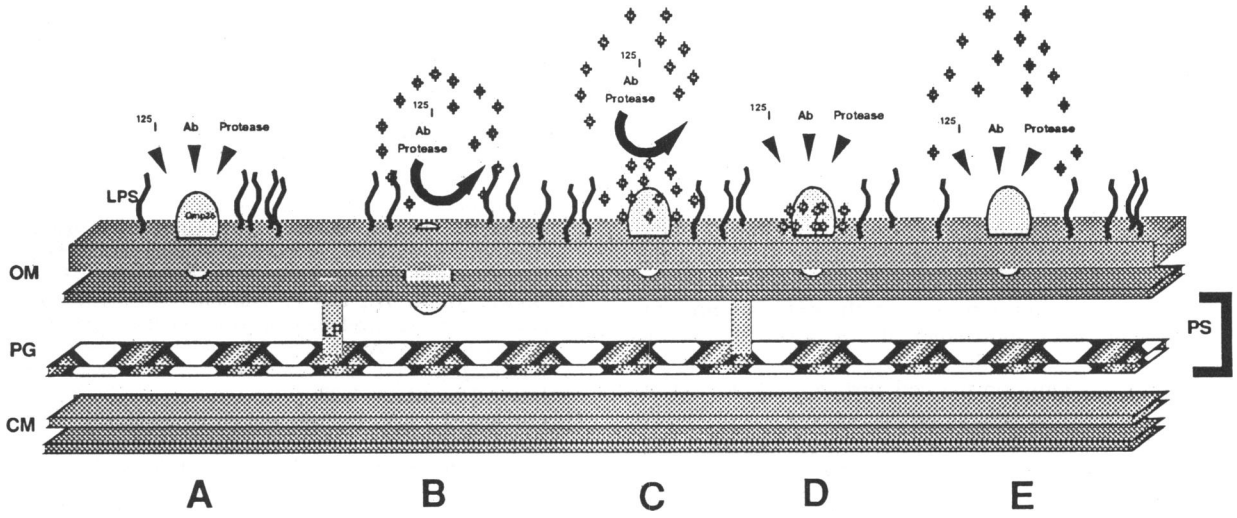

FIG. 12. Diagrammatic representation of Omp26 mobilization across the *P. gingivalis* outer membrane. Under hemin-deprived conditions (A), Omp26 was found predominantly in the outer aspect of the outer membrane exposed to the environment and was readily detected by ^{125}I, antibody (Ab), and protease. Growth of *P. gingivalis* in the presence of excess hemin (B) resulted in movement of Omp26 into the interior of the outer membrane or into the periplasmic space, where it was inaccessible to the probes used in this study. Under hemin-excess conditions, Omp26 could also become covered by hemin molecules, shielding it from exposure to ^{125}I, protease, or antibody (C). After heat shock treatment of hemin-excess-grown *P. gingivalis*, Omp26 appears on the surface and is detected by the localization probes (D). However, heat shock treatment could alter the hemin-binding capability of Omp26 so that it was no longer shielded by hemin, permitting access of the localization probes (E). OM, outer membrane; PG, peptidoglycan; CM, cytoplasmic membrane; PS, periplasmic space; LPS, lipopolysaccharide; LP, lipoprotein. Hemin is represented by black stars.

stresses have been shown to induce the production of heat shock proteins in eubacteria. Exposure of *Salmonella typhimurium* to oxidative stress results in the expression of at least five hydrogen peroxide-inducible proteins which appear to be identical to the proteins induced by heat shock (28). Acid shock of *E. coli* results in the synthesis of 16 acid-inducible proteins, 4 of which correspond to heat shock proteins (20). Although de novo induction of Omp26 may not be required for transmembrane mobilization, the appearance of Omp26 occurs in *P. gingivalis* after heat shock as well as during a hemin stress. Our findings indicate that Omp26 may not be a member of the heat shock protein family, since we have not shown its de novo synthesis in response to thermal stress but have demonstrated that it is constitutively found in the outer membrane, changing location in response to thermal stress and environmental hemin concentration. However, in contrast to the modulation by hemin, Omp26 is irreversibly mobilized to the cell surface after exposure to thermal stress.

A diagrammatic representation of Omp26 translocation in *P. gingivalis*, derived from the studies reported here, is presented in Fig. 12. Under hemin-deprived conditions, Omp26 was expressed on the *P. gingivalis* cell surface (Fig. 12A). In the presence of excess hemin, the Omp appeared to have migrated either into the inner aspect of the outer membrane or into the periplasmic space (Fig. 12B), since treatment of the cells with ^{125}I, trypsin, proteinase K, or specific antibody resulted in little to no probe reactivity. Importantly, the thin-section immunogold localization experiments would also suggest that Omp26 was partially internalized into the outer membrane, but this observation still remains equivocal. It was also possible that in conditions of hemin excess, Omp26 was completely shielded by hemin (Fig. 12C) and therefore was not detected by the three probes used in this study, giving rise to the idea that it was lost from the outer membrane surface. However, the fact that Omp26 was not removed from the surface after heat shock treatment and was identified by ^{125}I labeling has important implications relative to our proposed model of Omp26 translocation (Fig. 12D and E). The findings presented in this study indicate that hemin is not covering Omp26, since it was detected on the surface of heat-shocked *P. gingivalis* cells by ^{125}I labeling even in the presence of hemin (Fig. 12D). Furthermore, Omp26 was also iodinated in hemin-deprived cells which were replenished with hemin after heat shock. Using the hemin-conjugated photoactivatable cross-linker sulfosuccinimidyl 2-(*p*-azidosalicylamido)ethyl-1,3′-dithiopropionate, we have determined that Omp26 binds to hemin (8). Therefore, it was also possible that hemin binding of Omp26 was adversely affected by heat shock treatment and hemin did not shield Omp26, thereby allowing access of the localization probes (Fig. 12E). However, we have determined that Omp26 does bind hemin in the presence of heat shock (8) and therefore the localization probes did have access to Omp26 after heat shock treatment, as represented in Fig. 12D. It is likely that hemin did not shield the localization probes used in this study, since Omp26, which binds to hemin, was detected by ^{125}I labeling on the *P. gingivalis* surface after heat shock treatment. Thus, we conclude from the evidence presented in this report that Omp26 was removed from the outer membrane surface after hemin repletion (Fig. 12B). The model of protein translocation proposed in Fig. 12A and B for *P. gingivalis* Omp26 may represent the most accurate representation of this transmembrane event. Since only heterologous protein import and export systems across the outer membrane have been described for prokaryotic organisms (33), our study represents the first report of a putative autologous outer membrane protein import-export system in eubacteria.

The forces which drive this transmembrane event in *P. gingivalis* remain to be determined. These observations represent the first demonstration of the regulation of the

expression of the *P. gingivalis* Omp26 in the presence of a hemin-replete environment when combined with a heat shock stress. Since we have observed that Omp26 was completely lost from the cell surface of hemin-deprived *P. gingivalis* in less than 1 min after hemin was added to the cells (Fig. 1), heat shock treatment may inactivate the event(s) responsible for mobilization of this Omp off the surface. Heat shock may also induce a global stress response in *P. gingivalis*, resulting in the appearance of Omp26 on the outer membrane surface, and concomitantly inactivate the process(es) responsible for mobilization of this Omp off the cell surface when hemin is present in the external environment. Since multiple environmental stresses result in the translocation of Omp26 to the *P. gingivalis* cell surface, the appearance of this Omp on the cell surface may be coordinately regulated by a global stress operon (26). Hemin uptake, therefore, may be the preferred iron transport system for *P. gingivalis*, and by employing a surface-exposed stress protein for hemin assimilation, it may be able to circumvent host recognition, since stress proteins are well conserved phylogentically (26). The evolution of this putative iron uptake system may be significant for biologic preservation of critical bacterial uptake systems.

While there are numerous reports of prokaryotic proteins which traverse the cytoplasmic membrane of prokaryotes (for a review, see reference 33), this is the first description of an autologous bacterial protein export-import system across the outer membrane, as well as the first known report of a prokaryotic Omp which appears to be imported or buried in the outer membrane leaflets under excess nutrient conditions. Since we have determined that this protein binds hemin (8), it is likely that Omp26 functions to transport hemin into the *P. gingivalis* cell interior, where hemin may be processed by additional proteins located within the periplasm (1). Omp26 may function as hemin relay system or shunt for transfer and storage of this important iron source.

ACKNOWLEDGMENTS

This research was supported in part by Public Health Service grants DE00152 and DE07267 and by University of California Academic Senate research funds. T. E. Bramanti was a Dentist-Scientist Awardee during the tenure of this research.

We thank Daniel Guerrero for excellent assistance with electron microscopy and photography, Karen Lucas for manuscript preparation, and Evangeline Leash for critical review of the manuscript.

REFERENCES

1. **Ames, G. F.-L.** 1986. Bacterial periplasmic transport systems: structure, mechanism, and evolution. Annu. Rev. Biochem. **55:**497–425.
2. **Berryman, M. A., and R. D. Rodewald.** 1990. An enhanced method for postembedding immunocytochemical staining which preserves cell membranes. J. Histochem. Cytochem. **38:**159–170.
3. **Blake, M. S., and E. C. Gotschlich.** 1987. Functional and immunologic properties of pathogenic *Neisseria* surface proteins, p. 377–400. *In* M. Inouye (ed.), Bacterial outer membranes as model systems. John Wiley & Sons, Inc., New York.
4. **Bostford, J. L.** 1990. Analysis of protein expression in response to osmotic stress in *Escherichia coli*. FEMS Microbiol. Lett. **60:**355–360.
5. **Bramanti, T. E., and S. C. Holt.** 1990. Iron-regulated outer membrane proteins in the periodontopathic bacterium, *Bacteroides gingivalis*. Biochem. Biophys. Res. Commun. **166:** 1146–1154.
6. **Bramanti, T. E., and S. C. Holt.** 1991. Roles of porphyrins and host iron transport proteins in regulation of growth in *Porphyromonas gingivalis* W50. J. Bacteriol. **173:**7330–7339.
7. **Bramanti, T. E., and S. C. Holt.** Effect of porphyrins and host iron transport proteins on outer membrane protein expression in *Porphyromonas* (*Bacteroides*) *gingivalis*: identification of a novel 26 kilodalton hemin-repressible surface protein. Microb. Pathog., in press.
8. **Bramanti, T. E., and S. C. Holt.** Unpublished data.
9. **Braun, V.** 1985. The iron transport system of *Escherichia coli*, p. 41–80. *In* A. N. Martonosi (ed.), The enzymes of biological membrane, vol. 3. Plenum Press, New York.
10. **Braun, V., and K. Hantke.** 1991. Genetics of bacterial iron transport, p. 107–138. *In* G. Winkelmann (ed.), Handbook of microbial iron chelates. CRC Press, Boca Raton, Fla.
11. **Brown, M. R. W., and P. Williams.** 1985. The influence of environment on envelope properties affecting survival of bacteria in infections. Annu. Rev. Microbiol. **39:**527–556.
12. **Bullen, J. J.** 1981. The significance of iron in infection. Rev. Infect. Dis. **3:**1127–1138.
13. **Carlsson, J., J. F. Hofling, and G. K. Sundqvist.** 1984. Degradation of albumin, haemopexin, haptoglobin and transferrin, by black-pigmented *Bacteroides* species. J. Med. Microbiol. **18:**39–46.
14. **Chu, L., T. E. Bramanti, J. E. Ebersole, and S. C. Holt.** 1991. Hemolytic activity in the periodontopathogen, *Porphyromonas gingivalis*: kinetics of enzyme formation and localization. Infect. Immun. **59:**1932–1940.
15. **Deneer, H. G., and A. A. Potter.** 1989. Effect of iron restriction on the outer membrane proteins of *Actinobacillus* (*Haemophilus*) *pleuropneumoniae*. Infect. Immun. **57:**798–804.
16. **Finkelstein, R. A., C. V. Sciortino, and M. A. McIntosh.** 1983. Role of iron in microbe-host interactions. Rev. Infect. Dis. **5:**S759–S777.
17. **Glynn, L. E., and M. W. Steward.** 1977. Role of conformation in antigenicity, p. 335–351. *In* L. E. Glynn and M. W. Steward (ed.), Immunochemistry: an advanced textbook. John Wiley & Sons, New York.
18. **Grenier, D., G. Chao, and B. C. McBride.** 1989. Characterization of sodium dodecyl sulfate-stable *Bacteroides gingivalis* proteases by polyacrylamide gel electrophoresis. Infect. Immun. **57:**95–99.
19. **Hanson, M. S., and E. J. Hansen.** 1991. Molecular cloning, partial purification, and characterization of a haemin-binding lipoprotein from *Haemophilus influenzae* type b. Mol. Microbiol. **5:**267–278.
20. **Heyde, M., and R. Portalier.** 1990. Acid shock proteins of *Escherichia coli*. FEMS Microbiol. Lett. **69:**19–26.
21. **Kabir, S.** 1981. Composition and immunochemical properties of outer membrane proteins of *Vibrio cholerae*. J. Bacteriol. **144:**382–389.
22. **Kay, H. M., A. J. Birss, and J. W. Smalley.** 1990. Haemagglutinating and haemolytic activity of the extracellular vesicles of *Bacteroides gingivalis* W50. Oral Microbiol. Immunol. **5:**269–274.
23. **Kay, W. W., B. M. Phipps, E. Ishigura, and T. J. Trust.** 1985. Porphyrin binding by the surface array virulence protein of *Aeromonas salmonicida*. J. Bacteriol. **164:**1332–1336.
24. **Kennell, W. L., and S. C. Holt.** 1990. Comparative studies of the outer membranes of *Bacteroides gingivalis*, strains ATCC 33277, W50, W83, 381. Oral Microbiol. Immunol. **5:**121–130.
25. **Kennell, W. L., and S. C. Holt.** 1991. Extraction, purification, and characterization of major outer membrane proteins from *Wolinella recta* ATCC 33238. Infect. Immun. **59:**3740–3749.
26. **Lindquist, S., and E. A. Craig.** 1988. The heat-shock proteins. Annu. Rev. Genet. **22:**631–677.
27. **Martinez, J. L., A. Delgado-Iribarren, and F. Baquero.** 1990. Mechanisms of iron acquisition and bacterial virulence. FEMS Microbiol. Rev. **75:**45–56.
28. **Morgan, R. W., M. F. Christman, F. S. Jacobson, G. Storz, and B. N. Ames.** 1986. Hydrogen peroxide-inducible proteins in *Salmonella typhimurium* overlap with heat shock and other stress proteins. Proc. Natl. Acad. Sci. USA **83:**8059–8063.
29. **Morton, D. J., and P. Williams.** 1989. Characterization of the outer membrane proteins of *Haemophilus parainfluenzae* expressed under iron-sufficient and iron-restricted conditions. J.

Gen. Microbiol. **135**:445–451.
30. **Neilands, J. B.** 1982. Microbial envelope proteins related to iron. Annu. Rev. Microbiol. **36**:285–309.
31. **Otto, B. R., M. Sparrius, A. M. J. J. Verweij-van Vaught, and D. M. MacLaren.** 1990. Iron-regulated outer membrane protein of *Bacteroides fragilis* involved in heme uptake. Infect. Immun. **58**:3954–3958.
32. **Payne, S. M.** 1988. Iron and virulence in the family *Enterobacteriaceae*. Crit. Rev. Microbiol. **16**:81–111.
33. **Pugsley, A. P., and M. Schwartz.** 1985. Export and secretion of proteins by bacteria. FEMS Microbiol. Rev. **32**:3–38.
34. **Reynolds, E. S.** 1963. The use of lead citrate at high pH as an electronopaque stain in electron microscopy. J. Cell Biol. **17**:208–212.
35. **Sigel, S. O., and S. M. Payne.** 1982. Effect of iron limitation on growth, siderophore production, and expression of outer membrane proteins of *Vibrio cholerae*. J. Bacteriol. **150**:148–155.
36. **Spence, J., A. Cegielska, and C. Georgopoulos.** 1990. Role of *Escherichia coli* heat-shock proteins DnaK and HtpG in response to nutritional deprivation. J. Bacteriol. **172**:7157–7166.
37. **Stugard, C. E., P. A. Daskaleros, and S. M. Payne.** 1989. A 101-kilodalton heme-binding protein associated with Congo red binding and virulence of *Shigella flexneri* and enteroinvasive *Escherichia coli* strains. Infect. Immun. **57**:3534–3539.
38. **Towbin, H., T. Staehelin, and J. Gordon.** 1984. Electrophoretic transfer of proteins from acrylamide gels to nitrocellulose sheets: procedure and some applications. Proc. Natl. Acad. Sci. USA **76**:4350–4354.
39. **Weinberg, A., and S. C. Holt.** 1991. Chemical and biological activities of a 64 kDa outer sheath protein from *Treponema denticola* strains. J. Bacteriol. **173**:6935–6947.
40. **Weinberg, E. D.** 1978. Iron and infection. Microbiol. Rev. **42**:45–66.
41. **Weinberg, E. D.** 1984. Iron withholding: a defense against infection and neoplasia. Physiol. Rev. **64**:65–102.
42. **Yatvin, M. B., A. W. Clark, and F. L. Siegel.** 1987. Major *Escherichia coli* heat-stress proteins do not translocate: implication for cell survival. Int. J. Biol. Relat. Stud. Phys. Chem. Med. **52**:603–613.